

Dynamic response assessment of floors under multi-pedestrian walking loads: probabilistic analysis

Elyas Bayat*, Federica Tubino

DICCA, University of Genoa, Via Montallegro 1, Genoa, 16145, Italy

ARTICLE INFO

Keywords:

Building Floors
Vibration Serviceability
Walking Load
Harmonic Load
Walking Path
Probabilistic Analysis
Monte Carlo Simulation
Multiple-Pedestrian
Power spectral Density
Spectral Load Model

ABSTRACT

The dynamic response assessment of floors subjected to multi-pedestrian walking loads becomes a critical area of research, as it directly impacts the safety, serviceability, and comfort of floors due to advancements in construction technology and the use of high-strength, flexible, lowly damped, and light-weight materials. The complexity of pedestrian-induced dynamic loads necessitates a probabilistic approach to understand and predict the performance of floors under such conditions. This paper investigates the dynamic response of floors subjected to multiple-pedestrian walking loads, taking into account the randomness of the walking path and walking load. The research focuses on probabilistic multi-pedestrian walking load scenarios and utilizes Monte Carlo simulations to analyze the modal loading. An analytical equivalent power spectral density function for the modal force, based on an existing modal force for footbridges, is proposed. Furthermore, a formula is developed to estimate the mean value of the peak acceleration response of floors. The total peak acceleration response is calculated using the square root of the sum of the squares technique. The findings of this study contribute to the advancement of simplified methods for predicting the dynamic response of floors under multiple-pedestrian walking loads. These methods can enhance the accuracy and reliability of vibration serviceability assessment for floor structures.


1. Introduction

The dynamic response assessment of floors under multi-pedestrian walking loads is a crucial aspect in the design and construction of contemporary office buildings and other civil engineering structures. The increasing use of large, slender, and lightweight floors has made footfall-induced vibrations a governing limit state [1, 2]. To ensure the serviceability and safety of these structures, it is essential to understand and predict the dynamic response of floors subjected to multi-pedestrian walking loads [3, 4].

Current guidelines for evaluating floor vibration performance based on walking pedestrians propose simplified methods using a single pedestrian represented as a fixed periodic load. However, real-life walking scenarios involve different excitation points for each footfall, leading to an insufficient number of steps to construct a complete resonant response. Correction factors are introduced to address these issues, but concerns about their reliability arise from the literature [5–7]. Researchers suggest integrating probabilistic approaches with simplified techniques [8, 9], yet the impact of variability in walking paths on floor dynamics is inadequately considered [10–14]. Additionally, the influence of multi-pedestrian loads on floor vibrations needs further exploration, as experimental results suggest they may induce higher vibrations compared to single pedestrian scenarios [15–18].

The assessment of vibration serviceability for floor structures under multi-pedestrian walking loads has predominantly focused on structures like footbridges. For instance, Piccardo and Tubino [19] introduced an equivalent spectral model to analyze the dynamic response of footbridges to normal unrestricted pedestrian traffic, considering sources of randomness such as pedestrian arrivals, step frequencies, velocities, force amplitudes, and pedestrian weights. Ferrarotti and Tubino [20] proposed a generalized equivalent spectral model of pedestrian-induced forces on footbridges for serviceability analysis under both unrestricted and crowded conditions. However, these studies assumed that the dynamic response of footbridges is mainly dominated by the vibration mode with a natural frequency close to the mean step frequency, neglecting the influences of higher walking harmonics on the modal force. To address this, Nimmen et al. [21] proposed a new approach for predicting the dynamic response of footbridges subjected to pedestrian

*Corresponding author

 elyas.bayat@edu.unige.it (E. Bayat); federica.tubino@unige.it (F. Tubino)

ORCID(s):

traffic, extending a spectral load model to account for multiple harmonics of the walking load and its application to arbitrary mode shapes.

Moreover, Shahabpoor et al. [22] introduced a method to evaluate the impact of walking traffic on structural vibrations in pedestrian structures such as footbridges and floors. The proposed method takes into account the natural variability of walking forces and human bodies, as well as their individual interaction with the structure at their moving location. However, the authors noted that the proposed method is not suitable for manual calculations, and it has some limitations. For example, it considers stationary individuals, so it does not account for the effects of walking path variability and gait parameters (e.g., walking speed and step length) in this study. Wang et al. [23] proposed a spectral model for crowd walking loads, assuming that individual pedestrian walking is a stochastic stationary process and the coherence function is independent of the distance among pedestrians. The model includes three different pedestrian densities and contains the first two harmonics of walking loads. Model parameters, except for unrestricted traffic, are determined from group walking tests. However, this study neglected the effect of higher harmonics of walking loads on the dynamic response of floor structures.

Despite these advances, there is a need to extend such approaches to floors and consider the complexities introduced by their bi-dimensional structure and multi-pedestrian walking loads [24–26]. Additionally, probabilistic multi-person loading models can enhance the reliability of vibration serviceability assessments for floor structures subjected to various walking load scenarios. Therefore, it is crucial to develop generalized and simplified methods that can predict dynamic responses effectively, while taking into account realistic walking load scenarios and accurately considering the effects of multiple pedestrians and their walking paths.

Thus, this paper focuses on investigating the dynamic response of floors subjected to multiple-pedestrian walking loads, while considering the stochastic nature of both walking paths and walking loads. The paper begins by presenting a comprehensive mathematical framework for calculating the floor response to multi-pedestrian walking loads. Subsequently, the modal walking load is analyzed using probabilistic methods, employing Monte Carlo simulations for numerical evaluation. Then, an analytical equivalent power spectral density function for the modal force is introduced. Finally, the dynamic response of floors under multiple pedestrian walking loads is thoroughly examined using the proposed equivalent spectral model of the modal force.

2. Analytical formulation

2.1. Equation of motion

Consider a rectangular floor represented as a 2-D linear elastic structural system, as shown in Fig. 1. The equation of motion governing the system is given by [27, 28]:

$$\nabla_o^4 q(x, y, t) + \chi(x, y) \dot{q}(x, y, t) + \mu(x, y) \ddot{q}(x, y, t) = f(x, y, t) \quad (1)$$

where $x \in [0, L_x]$ and $y \in [0, L_y]$ are the coordinates of a point on the floor, t is the time, q represents the vertical deflection, f is the external load, χ is the damping coefficient, μ is the mass per unit area, and ∇_o^4 is a biharmonic operator. For an orthotropic plate, the biharmonic operator is expressed as:

$$\nabla_o^4 = D_x \frac{\partial^4}{\partial x^4} + 2H \frac{\partial^4}{\partial x^2 \partial y^2} + D_y \frac{\partial^4}{\partial y^4} \quad (2)$$

in which D_x and D_y are the flexural stiffnesses with respect to the x and y axes, respectively, while H represents the torsional stiffness. It is worth noting that for isotropic plates, $D_x = D_y = H$ [29].

For the multi-pedestrian walking load (Fig. 1), the exerted force is expressed as a summation of walking force of each pedestrian, modeled as moving multi-harmonic loads:

$$f(x, y, t) = \sum_{i=1}^{N_p} \sum_{h=1}^{N_h} G_i \alpha_{h_i} \sin\left(2\pi h f_{p_i} t + \phi_{h_i}\right) \delta\left(x - x_{p_i}(t)\right) \delta\left(y - y_{p_i}(t)\right) \times \left[H(t - \tau_i) - H\left(t - \tau_i - \frac{L_w p_i}{c_i}\right) \right] \quad (3)$$

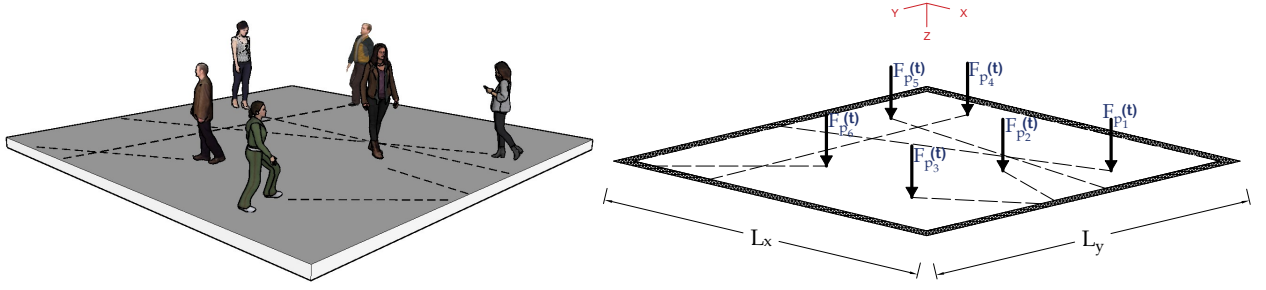


Figure 1: Modeling multi-pedestrian walking load on a rectangular floor

where G_i is the weight, f_{p_i} is the step frequency, τ_i is the arrival time, L_{wp_i} is the walking path length, c_i is the walking speed of the i -th pedestrian. Moreover, the parameters α_{hi} and ϕ_{hi} are the Dynamic Load Factor (DLF) and phase angle corresponding to h -th walking harmonic of the i -th pedestrian, respectively. In addition, $\delta()$ and $H()$ are the Dirac function and the Heaviside function, respectively. Moreover, $(x_{p_i}(t), y_{p_i}(t))$ is the location of the i -th pedestrian on the floor at the time t that is expressed as:

$$\begin{aligned} x_{p_i}(t) &= x_{0_i} + (c_i \cos \theta_i) t \\ y_{p_i}(t) &= y_{0_i} + (c_i \sin \theta_i) t \end{aligned} \quad (4)$$

where, (x_{0_i}, y_{0_i}) is the initial location of the i -th pedestrian on the floor and θ_i is the walking path angle with respect to x -axis corresponding to the i -th pedestrian.

By applying the modal coordinate transformation, the vertical deflection of the floor can be expressed as [30, 31]:

$$q(x, y, t) = \sum_{j=1}^{\infty} \sum_{k=1}^{\infty} \varphi_{j,k}(x, y) p_{j,k}(t) = \sum_{j=1}^{\infty} \sum_{k=1}^{\infty} \varphi_j(x) \varphi_k(y) p_{j,k}(t) \quad (5)$$

where $\varphi_{j,k}(x, y)$ is the j, k -th modal shape function, and $p_{j,k}(t)$ is the corresponding principal coordinate. Assuming proportional damping, the equation of motion of the j, k -th modal coordinate $\ddot{p}_{j,k}$ is given by:

$$\ddot{p}_{j,k}(t) + 2\xi_{j,k}\omega_{j,k}\dot{p}_{j,k}(t) + \omega_{j,k}^2 p_{j,k}(t) = \frac{1}{M_{j,k}} F_{j,k}(t) \quad (6)$$

in which:

$$F_{j,k}(t) = \int_0^{L_x} \int_0^{L_y} f(x, y, t) \varphi_{j,k}(x, y) dx dy \quad (7)$$

where $\xi_{j,k}$, $M_{j,k}$, $F_{j,k}(t)$, and $\omega_{j,k}$ is the j, k -th modal damping ratio, modal mass, modal force, and natural circular frequency, respectively. The modal force can be rewritten as follows by substituting Eq. 3 in Eq. 7:

$$\begin{aligned} F_{j,k}(t) &= \sum_{i=1}^{N_p} \sum_{h=1}^{N_h} G_i \alpha_{hi} \sin(2\pi h f_{p_i} t + \phi_h) \varphi_{j,k} \left(x_{0_i} + (c_i \cos \theta_i) t, y_{0_i} + (c_i \sin \theta_i) t \right) \\ &\times \left[H(t - \tau_i) - H\left(t - \tau_i - \frac{L_{wp_i}}{c_i}\right) \right] \end{aligned} \quad (8)$$

In order to perform a probabilistic analysis on the dynamic response of floors excited by multiple walking pedestrians, the random parameters corresponding to the modal force (Eq. 8) are defined from the probabilistic point

of view. In this regard, the walking load parameters such as G_i , α_{hi} , f_{pi} , and c_i are assumed to be normally distributed random variables defined as:

$$\begin{aligned} G &\sim \mu_G (1 + V_G N(0, 1)) \\ \alpha_h &\sim \mu_{\alpha_h} (1 + V_{\alpha_h} N(0, 1)) \\ f_p &\sim \mu_{f_p} (1 + V_{f_p} N(0, 1)) \\ c &\sim \mu_c (1 + V_c N(0, 1)) \end{aligned} \quad (9)$$

where μ_r and V_r ($r = G, \alpha_h, f_p, c$) represent the mean value and the coefficient of variation of the random variables, respectively. $N(0, 1)$ is the standard normal random variable. The phase angle ϕ_{hi} is assumed to be a uniform random variable in $[0, 2\pi]$.

It is assumed that the arrival of pedestrians on the floor follows a Poisson process with a constant average rate λ of events (arrivals) occurring per unit time. Then, the time lag between two consequent pedestrian τ has an exponential distribution with parameter λ as:

$$\tau \sim Exp(\lambda); \quad (\lambda = \frac{E[L_{wp}]}{E[c]}) \quad (10)$$

where $E[L_{wp}]$ and $E[c]$ are the mean value of the walking path length and of the pedestrian walking speed, respectively. Therefore, the arrival time of the i -th pedestrian can be expressed as:

$$\tau_i = \frac{\lambda}{N_p} \sum_{k=1}^i Exp_k(1) \quad (11)$$

where $Exp_k(1)$ are exponential random variables with unitary return period.

The random parameters related to the walking path are assumed to have uniform distributions in certain ranges based on the loading scenarios that have been defined. According to Fig. 2, two multi-pedestrian loading scenarios are considered in this paper to assess the dynamic response of floors. For the first multi-pedestrian loading scenario (MLS1), it is assumed that the pedestrians start walking from different points at two sides of floor parallel to the x -axis ($\theta \in \{0, 2\pi\}$, $x_{0i} \in \{0, L_x\}$, $y_{0i} \in [0, L_y]$). In the second multi-pedestrian loading scenario (MLS2), the pedestrians are assumed to start walking from different points on all sides of the floor with different walking path angles ($\theta \in [0, 2\pi]$, $x_{0i} \in [0, L_x]$, $y_{0i} \in [0, L_y]$). The parameters related to the initial location of the pedestrians and walking path angles can be expressed mathematically as follows:

$$\begin{aligned} MLS1 : \theta &\in \{0, 2\pi\}; \quad x_0 \in \{0, L_x\}; \quad y_0 \in [0, L_y] \\ MLS2 : \theta &\in [0, 2\pi]; \quad x_0 \in [0, L_x]; \quad y_0 \in [0, L_y] \end{aligned} \quad (12)$$

Let us assume a floor as an ideal simply supported rectangular floor:

$$\varphi_{j,k}(x, y) = \varphi_j(x) \varphi_k(y) = \sin\left(\frac{j\pi x}{L_x}\right) \sin\left(\frac{k\pi y}{L_y}\right) \quad (13)$$

The modal force (Eq. 7) can be expressed as follows:

$$F_{j,k}(t) = \sum_{i=1}^{N_p} \sum_{h=1}^{N_h} G_i \alpha_{hi} \sin(2\pi h f_{pi} t + \phi_{hi}) \sin\left(\frac{j\pi (x_{0i} + (c_i \cos\theta_i) t)}{L_x}\right) \sin\left(\frac{k\pi (y_{0i} + (c_i \sin\theta_i) t)}{L_y}\right)$$

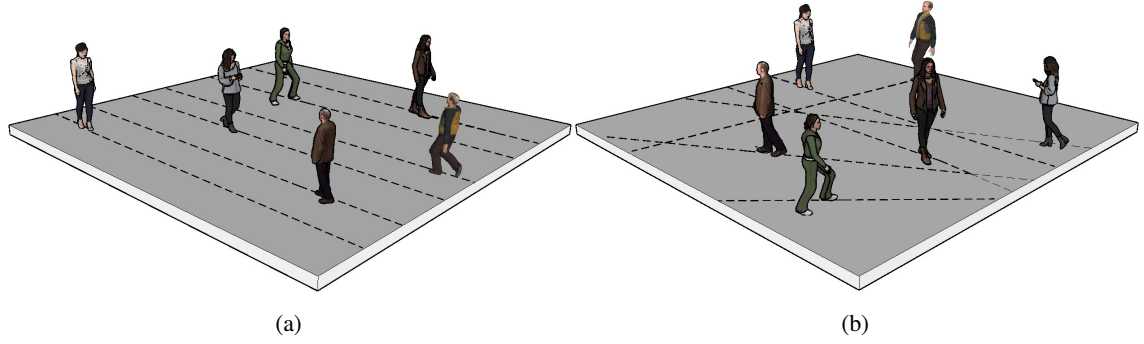


Figure 2: Multi-pedestrian loading scenarios: (a) MLS1 (b) MLS2

$$\times \left[H(t - \tau_i) - H\left(t - \tau_i - \frac{L_{wp_i}}{c_i}\right) \right] \quad (14)$$

Taking into account only the walking harmonic h , the modal force of multiple pedestrians due to the walking harmonic h can be expressed in non-dimensional form as:

$$\begin{aligned} \tilde{F}_{h,j,k}(\tilde{t}) = & \sum_{i=1}^{N_p} \frac{\tilde{G}_i \tilde{\alpha}_{h_i}}{4} \left[\sin\left(\beta_{1,h,j,k_i} \tilde{t} - \phi_{j,\tilde{x}_{0i}} + \phi_{k,\tilde{y}_{0i}} + \phi_{h_i}\right) - \sin\left(\beta_{2,h,j,k_i} \tilde{t} - \phi_{j,\tilde{x}_{0i}} - \phi_{k,\tilde{y}_{0i}} + \phi_{h_i}\right) - \right. \\ & \left. - \sin\left(\beta_{3,h,j,k_i} \tilde{t} + \phi_{j,\tilde{x}_{0i}} + \phi_{k,\tilde{y}_{0i}} + \phi_{h_i}\right) + \sin\left(\beta_{4,h,j,k_i} \tilde{t} + \phi_{j,\tilde{x}_{0i}} - \phi_{k,\tilde{y}_{0i}} + \phi_{h_i}\right) \right] \quad (15) \\ & \times \left[H(\tilde{t} - \tilde{\tau}_i) - H\left(\tilde{t} - \tilde{\tau}_i - \frac{\pi \tilde{L}_{wp_i}}{\tilde{\Omega}_{h,j,k_i} \tilde{\Omega}_{c,h_i}}\right) \right] \end{aligned}$$

where:

$$\begin{aligned} \beta_{1,h,j,k_i} &= \tilde{\Omega}_{h,j,k_i} \left[1 - \tilde{\Omega}_{c,h_i} \left(j \cos \theta_i - \frac{k \sin \theta_i}{\rho} \right) \right], \\ \beta_{2,h,j,k_i} &= \tilde{\Omega}_{h,j,k_i} \left[1 - \tilde{\Omega}_{c,h_i} \left(j \cos \theta_i + \frac{k \sin \theta_i}{\rho} \right) \right], \\ \beta_{3,h,j,k_i} &= \tilde{\Omega}_{h,j,k_i} \left[1 + \tilde{\Omega}_{c,h_i} \left(j \cos \theta_i + \frac{k \sin \theta_i}{\rho} \right) \right], \\ \beta_{4,h,j,k_i} &= \tilde{\Omega}_{h,j,k_i} \left[1 + \tilde{\Omega}_{c,h_i} \left(j \cos \theta_i - \frac{k \sin \theta_i}{\rho} \right) \right], \\ \phi_{j,\tilde{x}_{0i}} &= j\pi \tilde{x}_{0i}; \quad \phi_{k,\tilde{y}_{0i}} = k\pi \tilde{y}_{0i} \end{aligned} \quad (16)$$

The non-dimensional quantities in Eqs. 15-16 are defined as follows:

$$\begin{aligned} \tilde{F}_{h,j,k} &= \frac{F_{h,j,k}}{\mu_G \mu_{\alpha_h}}; \quad \tilde{\Omega}_{h,j,k_i} = \frac{2\pi h f_{p_i}}{\omega_{j,k}}; \quad \tilde{\Omega}_{c,h_i} = \frac{c_i}{2h f_{p_i} L_x}; \\ \tilde{\alpha}_{h_i} &= \frac{\alpha_{h_i}}{\mu_{\alpha_h}}; \quad \tilde{G}_i = \frac{G_i}{\mu_G}; \\ \tilde{t} &= \omega_{j,k} t; \quad \tilde{\tau}_i = \omega_{j,k} \tau_i; \\ \tilde{x}_{0i} &= \frac{x_{0i}}{L_x}; \quad \tilde{y}_{0i} = \frac{y_{0i}}{L_y}; \quad \rho = \frac{L_y}{L_x} \end{aligned} \quad (17)$$

To analyze the modal force and dynamic response of floors using non-dimensional parameters, the mean values of the non-dimensional frequency ratio and pedestrian speed parameters are defined as follows:

$$\mu_{\tilde{\Omega}_{h,j,k}} = \frac{2\pi h \mu_{f_p}}{\omega_{j,k}}; \quad \mu_{\tilde{\Omega}_{c,h}} = \frac{\mu_c}{2h \mu_{f_p} L_x} \quad (18)$$

The equation of motion of the $j, k - th$ principal coordinate due to the single walking harmonic h can be expressed as:

$$\ddot{\tilde{p}}_{h,j,k}(\tilde{t}) + 2\tilde{\xi}_{j,k} \dot{\tilde{p}}_{h,j,k}(\tilde{t}) + \tilde{p}_{h,j,k}(\tilde{t}) = \tilde{F}_{h,j,k}(\tilde{t}) \quad (19)$$

in which:

$$\tilde{p}_{h,j,k}(\tilde{t}) = \frac{M_{j,k}}{\mu_G \mu_{\alpha_h}} \tilde{p}_{h,j,k}(\tilde{t}) \quad (20)$$

2.2. Power Spectral Density function of dynamic response

The Power Spectral Density (PSD) function of modal acceleration response of floors can be calculated based on the PSD of modal force and expressed in non-dimensional form as follows [32, 33]:

$$S_{\ddot{\tilde{p}}_{h,j,k}}(\tilde{\Omega}) = \left| H_{\ddot{\tilde{p}}_{j,k}}(\tilde{\Omega}) \right|^2 S_{\tilde{F}_{h,j,k}}(\tilde{\Omega}) \quad (21)$$

where $H_{\ddot{\tilde{p}}_{j,k}}(\tilde{\Omega})$ is the acceleration Frequency Response Function (FRF) of the $j, k - th$ non-dimensional modal coordinate. Assuming a linear structural system with classical viscous damping, the FRF function is given by:

$$H_{\ddot{\tilde{p}}_{j,k}}(\tilde{\Omega}) = \frac{-\tilde{\Omega}^2}{1 - \tilde{\Omega}^2 + 2i\tilde{\xi}_{j,k}\tilde{\Omega}} \quad (22)$$

where $\tilde{\Omega}$ denotes the non-dimensional circular frequency, and i represents the imaginary unit.

2.3. Maximum dynamic response

The mean value of the non-dimensional modal peak acceleration of floors induced by multi pedestrian walking loads can be estimated as follow by assuming the modal force as a stationary random process [34]:

$$\ddot{\tilde{p}}_{h,j,k_{max}} = g_{\tilde{p}_{j,k}} \sigma_{\tilde{p}_{h,j,k}} \quad (23)$$

where $g_{\tilde{p}_{j,k}}$ is the peak factor and $\sigma_{\tilde{p}_{h,j,k}}$ is the standard deviation of the non-dimensional acceleration response. By assuming that the dynamic response of floors for the mode j, k is primarily resonant due to the $h - th$ harmonic, the variance of the non-dimensional acceleration response can be estimated as [33]:

$$\sigma_{\tilde{p}_{j,k}}^2 \cong \frac{\pi S_{\tilde{F}_{h,j,k}}(1)}{4\tilde{\xi}_{j,k}} \quad (24)$$

where $S_{\tilde{F}_{h,j,k}}(1)$ is the PSD of the non-dimensional modal force at $\tilde{\Omega} = 1$ which indicates the resonant condition due to the $h - th$ harmonic ($\omega_{j,k} = 2\pi h f_p$). Moreover, the peak coefficient, which is a non-dimensional quantity referred to the amplification of the dynamic response of a structure subjected to stationary random excitation, is defined as follows [35]:

$$g_{\ddot{p}_{j,k}} = \sqrt{2 \ln \left(2 v_{\ddot{p}_{j,k}}^e \tilde{T} \right)} + \frac{0.5772}{\sqrt{2 \ln \left(2 v_{\ddot{p}_{j,k}}^e \tilde{T} \right)}} \quad (25)$$

in which \tilde{T} is the mean value of the non-dimensional time length that N_p pedestrians are crossing on the floor and calculated using the following formula:

$$\tilde{T} = \frac{\omega_{j,k} N_p E [L_{wp}]}{\mu_c} \quad (26)$$

The term $E [L_{wp}]$ represents the mean value of the walking path length crossed by each pedestrian. Additionally, $v_{\ddot{p}_{j,k}}^e$ corresponds to the reduced expected frequency and is given by:

$$v_{\ddot{p}_{j,k}}^e = \left(1.63 q_{\ddot{p}_{j,k}}^{0.45} - 0.35 \right) v_{\ddot{p}_{j,k}} \quad (27)$$

$$v_{\ddot{p}_{j,k}} \cong \frac{1}{2\pi}$$

where $v_{\ddot{p}_{j,k}}$ is the expected frequency of the non-dimensional modal acceleration response. Furthermore, $q_{\ddot{p}_{j,k}}$ is the spectral bandwidth parameter, which can be estimated under the assumption that $\xi_{j,k} \ll 1$, as follows:

$$q_{\ddot{p}_{j,k}} \cong 2 \sqrt{\frac{\xi_{j,k}}{\pi}} \quad (28)$$

The mean value of the maximum modal acceleration response for the $j, k - th$ mode, excited under resonant conditions by the $h - th$ walking harmonic, can be calculated in dimensional form as follows:

$$\ddot{p}_{j,k,max} = \frac{\mu_G \mu_{\alpha_h}}{M_{j,k}} \ddot{p}_{h,j,k,max} \quad (29)$$

It should be recalled that the maximum modal acceleration response calculated by Eq. 29 is based on the assumption that the modal dynamic response corresponding to mode j, k is mainly governed by the walking harmonic h , and the contribution of the other walking harmonics is negligible.

The mean value of the maximum modal acceleration response for the mode j, k can be expressed in the physical coordinates as follows:

$$\ddot{q}_{j,k,max}(x, y) = \ddot{p}_{j,k,max} \phi_{j,k}(x, y) \quad (30)$$

Finally, to consider the effect of various modes on the maximum acceleration response of floors at (x, y) , the Square Root of Sum of Squares (SRSS) technique can be used, assuming that the modes are well-separated [32]:

$$\ddot{q}_{max}(x, y) = \sqrt{\sum_{j=1}^{N_j} \sum_{k=1}^{N_k} \left(\ddot{q}_{j,k,max}(x, y) \right)^2} \quad (31)$$

where N_j and N_k represent the mode numbers considered along the x and y axes, respectively.

3. Numerical analysis: Monte Carlo simulations

In this section, the multi-pedestrian walking loads in both the time and frequency domains are examined. To analyze the modal force (Eq. 15) using a probabilistic approach with Monte Carlo simulations, the following mean values (μ) and coefficient of variation (V) are assumed for the parameters defined in Eq. 9, are considered [36, 37]:

$$\begin{aligned}
 \mu_G &= 750 \text{ N}; & V_G &= 0.17 \\
 \mu_{f_p} &= 1.87 \text{ Hz}; & V_{f_p} &= 0.1 \\
 \mu_c &= 1.327 \frac{\text{m}}{\text{s}^2}; & V_c &= 0.11 \\
 \mu_{\alpha_1} &= 0.356; & V_{\alpha_1} &= 0.16 \\
 \mu_{\alpha_2} &= 0.07; & V_{\alpha_2} &= 0.43 \\
 \mu_{\alpha_3} &= 0.05; & V_{\alpha_3} &= 0.4 \\
 \mu_{\alpha_4} &= 0.05; & V_{\alpha_4} &= 0.4 \\
 \mu_{\alpha_5} &= 0.03; & V_{\alpha_5} &= 0.5
 \end{aligned} \tag{32}$$

It should be noted that in order to satisfy the stationarity hypothesis, the walking of multiple pedestrians is repeated 10 times for each simulation. This repeated process enables the simulation achieve a level of statistical significance that is reliable in the context of the stationary hypothesis.

Fig. 3 represents the time history of the modal force of multi-pedestrian walking load due to walking harmonic h , obtained from a Monte Carlo simulation assuming the random loading scenarios MLS1 (Fig. 3a) and MLS2 (Fig. 3b).

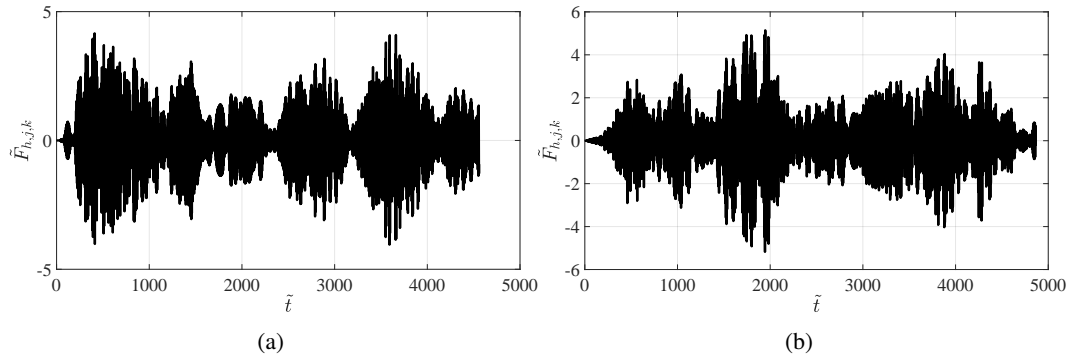


Figure 3: Time history of the modal force due to the walking harmonic h , loading scenarios: (a) MLS1 (b) MLS2, ($j = k = 1$, $\rho = 1$, $\mu_{\tilde{\Omega}_{c,h}} = 0.005$, $h = 4$, and $N_p = 10$)

According to Eq. 15, the modal force due to the walking harmonic h is dependent on different random variables. To assess the effect of different random variables on the modal force, the Power Spectral Density (PSD) function of the modal force can be estimated taking into account different values for the involved parameters such as $\tilde{\Omega}_{c,h}$, the aspect ratio (ρ), the loading scenario (MLS1 and MLS2), and the number of pedestrians (N_p).

The PSD of the modal force is estimated using Welch's method, which is a widely used spectral estimation technique in signal processing [38]. The method divides the signal into overlapping segments, applies a window function to each segment to reduce spectral leakage, and computes the periodogram of each segment. The individual periodograms are then averaged to obtain a smoothed estimate of the PSD. In this study, the PSD of the modal force is estimated by performing 10,000 Monte Carlo simulations for each analysis. Moreover, the 'pwelch' function in MATLAB is used to calculate the PSD, applying a Hanning window with 50% overlap to each segment and setting the segment length to 4096 samples with a sampling period $T_s = 0.01$ (sec).

3.1. Effect of $\tilde{\Omega}_{c,h}$ on the PSD of modal force

In this section, the effect of the variability of $\tilde{\Omega}_{c,h}$ on the PSD function of the modal force is examined. Fig. 4, plots the PSD functions of the modal force due to the walking harmonic h , considering different values for the mean value

of $\tilde{\Omega}_{c,h}$ and h . The results show that the PSD function of the modal force is not affected by the variability of $\tilde{\Omega}_{c,h}$ for different walking harmonic orders.

Moreover, Fig. 5, shows the superimposition of the PSD functions of the modal force and the PDFs of walking frequency due to different walking harmonics. According to Fig. 5, it can be seen that the PSD function of the modal force is mainly governed by the variability of the step frequency (f_p) and its corresponding distribution is proportional to the probability density function (PDF) of the $h - th$ harmonic of the step frequency:

$$S_{\tilde{F}_{h,j,k}}(\tilde{\Omega}) \propto p_{hf_p}(\tilde{\Omega}) \quad (33)$$

where $\tilde{\Omega}$ is the non-dimensional circular frequency.

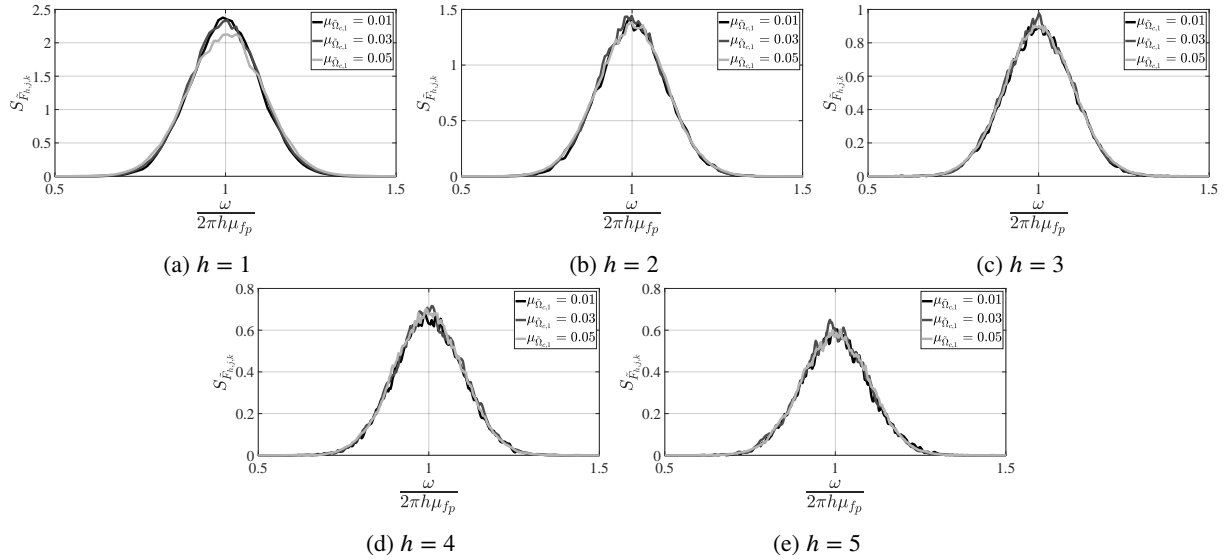


Figure 4: PSD functions of the non-dimensional modal force ($N_p = 10$) due to the loading scenario MLS2 for different $\mu_{\tilde{\Omega}_{c,1}}$: $\rho = 1$, $j = k = 1$, (a) $h = 1$, (b) $h = 2$, (c) $h = 3$, (d) $h = 4$, and (e) $h = 5$

In addition, as depicted in Fig. 5, it can be observed that the amplitude of the PSD function of the modal force varies with different walking harmonic orders. In simpler terms, the PSD function of the modal force is proportional to the variability of dynamic load factor (DLF) of the corresponding walking harmonic h .

In order to assess the contribution of all walking harmonics in the PSD function of the modal force, Fig. 6 shows the PSD function of the dimensional modal force taking into account all the walking harmonics. The graph shows that the higher walking harmonics give less energy to the floor system that is due to the fact that the mean value of DLF for the first walking harmonic is much higher than corresponding values for the higher walking harmonics. In addition, the distribution of the PSD function of the non-dimensional modal force indicates that by considering five walking harmonic orders ($N_h = 5$), the resonant condition can be provided for floors which have the natural frequencies lower than around 12 Hz.

3.2. Effect of aspect ratio (ρ) on the PSD of modal force

In this section, the PSD function of the non-dimensional force is investigated considering floors with different aspect ratios (ρ). Fig. 7 plots the PSD function of the non-dimensional modal force varying the aspect ratio (ρ) for different walking harmonics. The results indicate that the PSD function of the non-dimensional modal force is not dependent on the aspect ratio.

3.3. Effect of the loading scenario on the PSD of the modal force

In this section, the effect of loading scenarios (MLS1 and MLS2) on the PSD of the modal force is investigated. Fig. 8 compares the PSD of the non-dimensional modal force for different walking harmonics under the MLS1 and

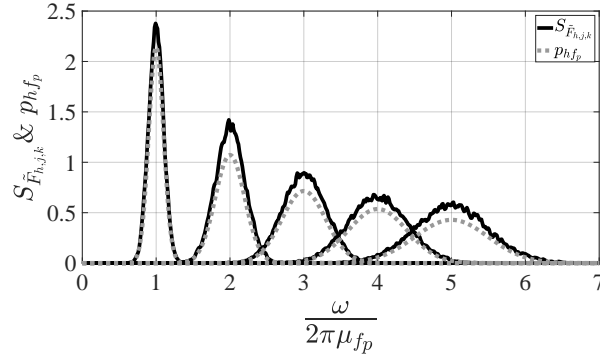


Figure 5: PSD function of the non-dimensional modal force and PDF of step frequency due to different walking harmonics (MLS2, $N_p = 10$, $\mu_{\tilde{\Omega}_{c,1}} = 0.01$, $\rho = 1$, $j = k = 1$)

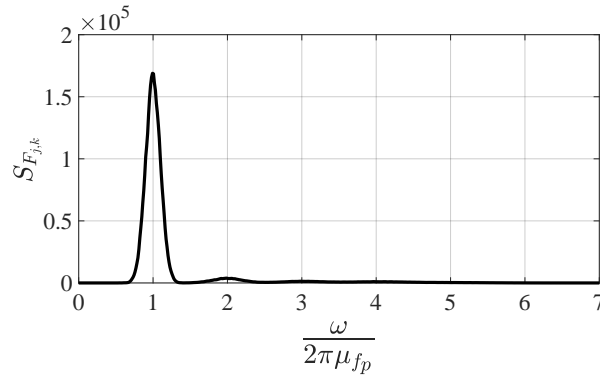


Figure 6: PSD function of the dimensional modal force due to all walking harmonics (MLS2, $N_p = 10$, $\mu_{\tilde{\Omega}_{c,1}} = 0.01$, $\rho = 1$, $j = k = 1$)

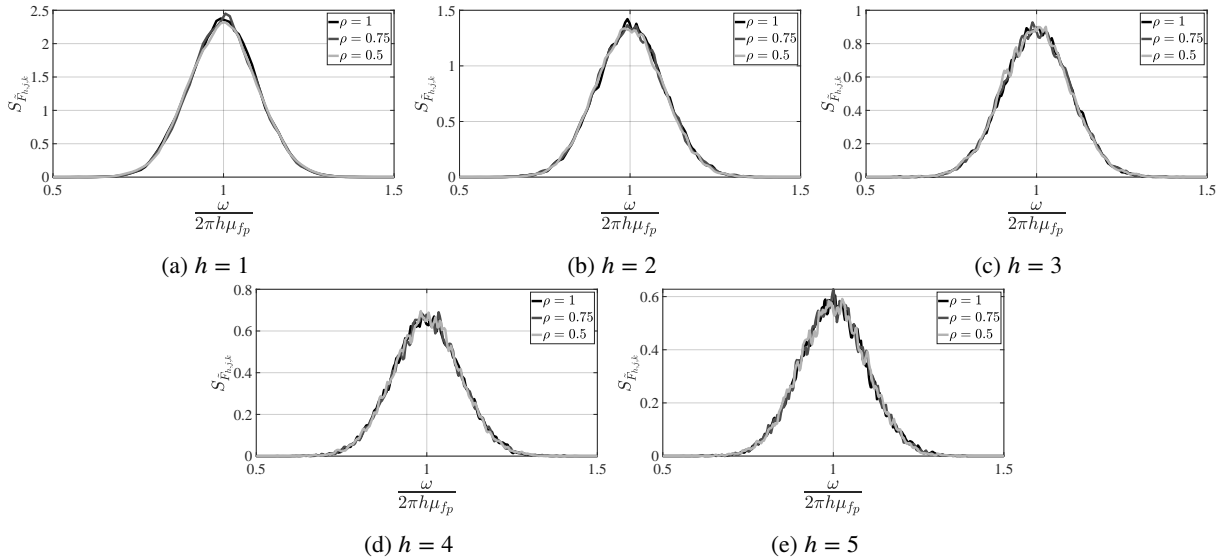


Figure 7: PSD functions of the non-dimensional modal force ($N_p = 10$) for different aspect ratios ρ : (MLS2, $\mu_{\tilde{\Omega}_{c,1}} = 0.01$, $j = k = 1$) (a) $h = 1$, (b) $h = 2$, (c) $h = 3$, (d) $h = 4$, and (e) $h = 5$

MLS2 loading scenarios. The analysis reveals that the amplitude of the PSD functions varies depending on the loading scenario, with the MLS1 scenario resulting in higher amplitudes than MLS2 at certain frequencies.

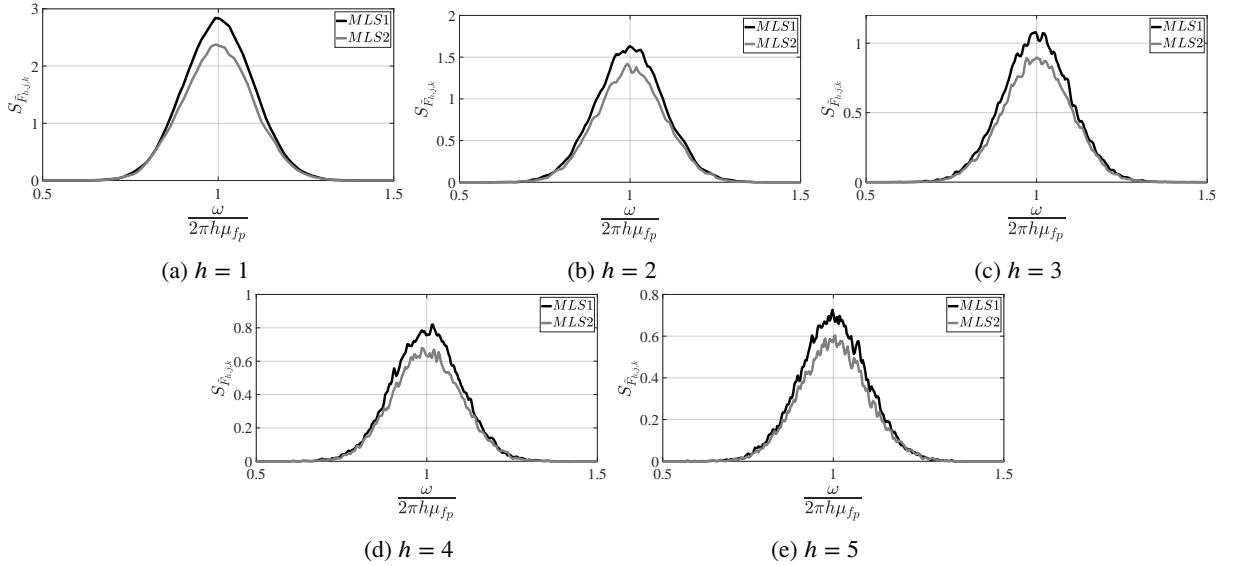


Figure 8: PSD functions of the non-dimensional modal force ($N_p = 10$) due to the loading scenarios MLS1 and MLS2: $\mu_{\tilde{\Omega}_{c,1}} = 0.01$, $\rho = 1$, $j = k = 1$, (a) $h = 1$, (b) $h = 2$, (c) $h = 3$, (d) $h = 4$, and (e) $h = 5$

The effect of the loading scenario on the PSD function of the modal force, can be analysed based on the mean value of the walking path length for the two scenarios. In order to assess the effect of the loading scenario on the PSD function of the modal force, the mean value of the walking path should be determined based on the Cartesian coordinates (x, y) , where the modal force is defined. In this regard, the coefficient C_{wp} is defined based on the mean value of walking path length (with respect to the main axes) in order to consider the effect of the loading scenarios on the PSD function of the modal force, which is given by:

$$C_{wp} = \sqrt{\frac{E[(L_{wp} \cos \theta)^2]}{L_x^2} + \frac{E[(L_{wp} \sin \theta)^2]}{L_y^2}} \quad (34)$$

For the loading scenario MLS1, since the pedestrians are crossing along the length of the floor, the walking path coefficient is equal to 1. Regarding to the loading scenario MLS2, according to the results shown in Fig. 9, which is obtained from the Monte Carlo simulations for floors with different aspect ratios, it can be observed that the square of the normalized mean values of the walking path length with respect to the main axes (x, y) vary linearly with respect to the aspect ratio (ρ) . Moreover, it can be seen that the summation of these two mean values is constant which means that the walking path coefficient (C_{wp}) has also a constant value for this loading scenario for floors with different aspect ratios.

Therefore, the results show that the PSD function of the modal force is proportional to the walking path coefficient (C_{wp}):

$$S_{\tilde{F}_{h,j,k}}(\tilde{\Omega}) \propto C_{wp} \quad (35)$$

where the coefficient of the walking path (C_{wp}) is defined as follows depending on the loading scenario:

$$C_{wp} = \begin{cases} 1; & \text{(MLS1)} \\ 0.8; & \text{(MLS2)} \end{cases} \quad (36)$$

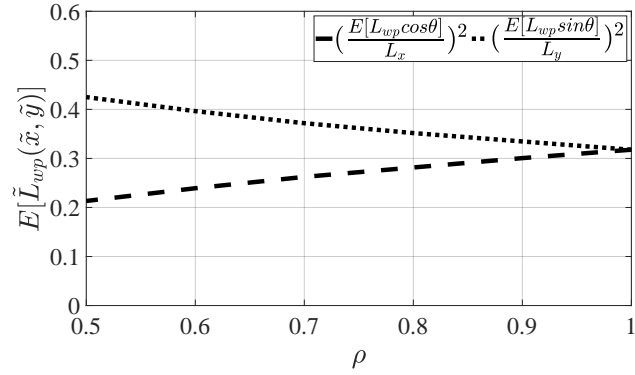


Figure 9: Square of the normalized mean values of the walking path length with respect to the main axes (x, y) for the loading scenario MLS2 varying aspect ratio (ρ)

3.4. Effect of the number of pedestrians (N_p) on the PSD function of the modal force

Fig. 10 shows the PSD function of the non-dimensional modal force for different walking harmonics taking into account different number of pedestrians. The results indicate that the amplitude of the PSD function the modal force at specific frequency is proportional to the total number of the pedestrians which are walking on the floor:

$$S_{\tilde{F}_{h,j,k}}(\tilde{\Omega}) \propto N_p \quad (37)$$

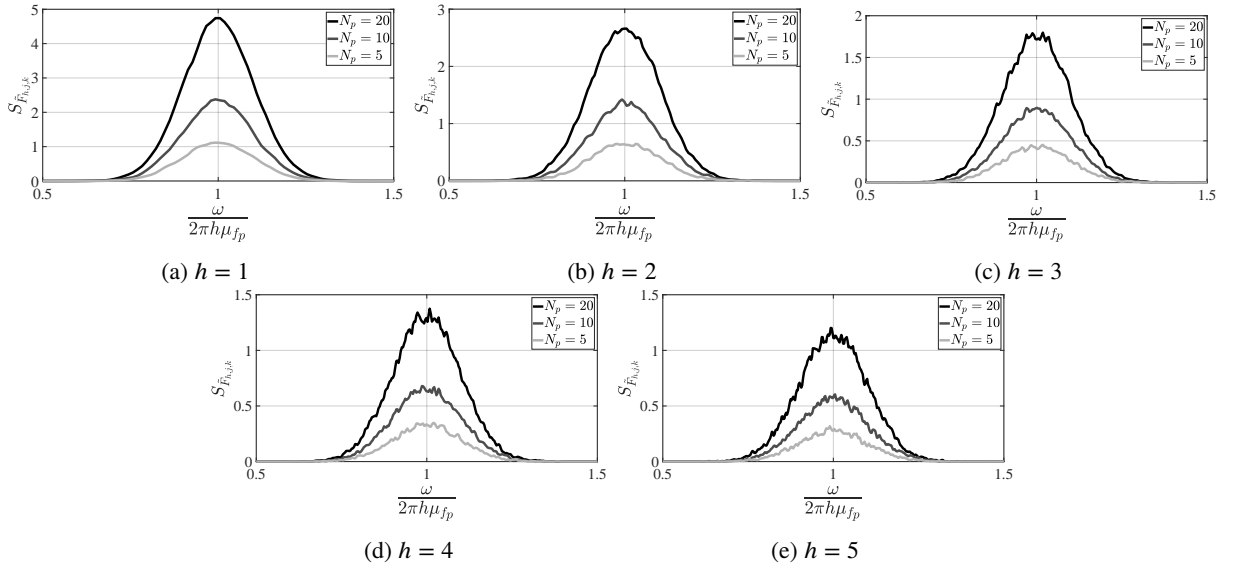


Figure 10: PSD functions of the non-dimensional modal force due to the loading scenarios MLS2 for different number of pedestrians: $\tilde{\Omega}_{c,1} = 0.01$, $\rho = 1$, $j = k = 1$, (a) $h = 1$, (b) $h = 2$, (c) $h = 3$, (d) $h = 4$, and (e) $h = 5$

4. Equivalent spectral load model

Equivalent spectral models can be used to simplify the analysis of complex dynamic systems by approximating their response to a given input using a set of simpler mathematical models. In the context of multi pedestrian walking loads, the equivalent spectral model can be used to model the modal forces generated by the pedestrians as they walk on a floor structures.

According to an equivalent spectral model of the modal force proposed by [19, 21] to assess the vibration serviceability of footbridges and the numerical analyses carried out in Sec. 3, the equivalent spectral model for the non-dimensional modal force is extended for VSA of building floors as follows:

$$S_{\tilde{F}_{h,j,k}}(\tilde{\Omega}) = \frac{N_p C_{wp} \mu_G^2 \mu_{\alpha_h}^2 (1 + V_h^2)}{2} \left[\frac{1}{\rho} \int_0^1 \int_0^\rho \phi_{j,k}^2(\tilde{x}, \tilde{y}) d\tilde{x} d\tilde{y} \right] p_{h f_p}(\tilde{\Omega}) \quad (38)$$

where V_h is the coefficient of variation of the product of random variables G and α_h . It is assumed that the random variables G and α_h act as a single random variable ($G\alpha_h$) [21, 39] which are statistically independent. The coefficient of variation V_h is given by:

$$V_h = \sqrt{V_{\alpha_h}^2 + V_G^2 + V_{\alpha_h}^2 V_G^2} \quad (39)$$

Moreover, $p_{h f_p}(\tilde{\Omega})$ is the non-dimensional PDF of the h – th harmonic of the step frequency which is given by:

$$p_{h f_p}(\tilde{\Omega}) = \frac{1}{\sqrt{2\pi}} e^{-\frac{1}{2} \left(\frac{\tilde{\Omega}-1}{V_{h f_p}} \right)^2} \quad (40)$$

The accuracy of the equivalent spectral model of the modal force is validated based on the numerical results obtained from the Monte Carlo simulations. For example, Fig. 11 compares the PSD of the non-dimensional modal force obtained from the numerical and analytical approaches for the loading scenarios MLS1 and MLS2. The results show that the PSD of the modal force is very well predicted by the analytical model.

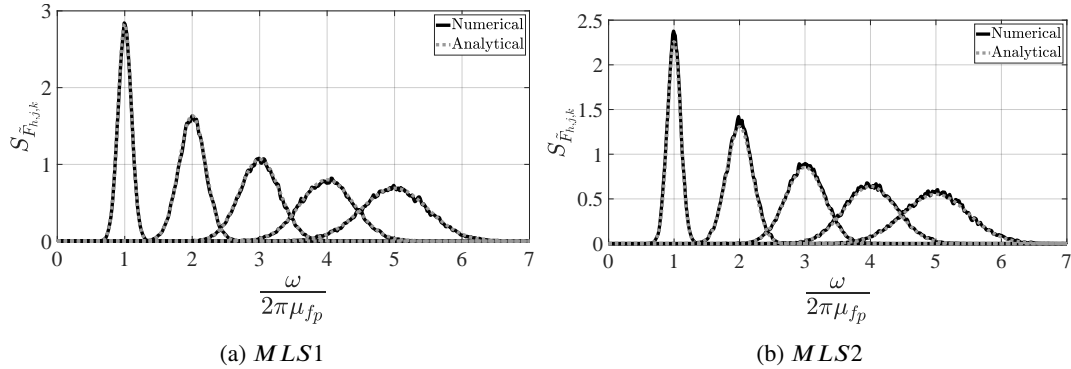


Figure 11: PSD of the modal force due to different walking harmonics: comparison of the numerical and analytical results ($N_p = 10$, $\tilde{\Omega}_{c,1} = 0.01$, $\rho = 1$, $j = k = 1$)

5. Estimation of peak acceleration response

In this section, the dynamic response of floors under random multi-pedestrian walking loads is investigated, exploring both the time and frequency domains. In time domain analysis, the dynamic response of the floors is evaluated by examining the time-dependent behavior of the floor system and the probability distribution of the maximum dynamic response. On the other hand, in frequency domain analysis, the dynamic response of the floors is evaluated by examining the power spectral density function of the dynamic response. Then, adopting the Davenport peak acceleration factor formulation [34] (Eq. 23), the mean value of the maximum dynamic response of the floor is estimated from the equivalent spectral model of the modal force.

5.1. Time domain analysis

In this section, the dynamic response of floors subjected to random multi-pedestrian walking loads is investigated using time domain analysis. Monte Carlo simulations are used to obtain the peak acceleration response for each simulation, which is derived from the time history acceleration response.

As an example, Fig. 12 shows the non-dimensional time history of the modal force and corresponding modal acceleration response of the vibration mode j, k -th, due to the walking harmonic h of multiple pedestrians obtained from a Monte Carlo simulation of the random loading scenario MLS2. Moreover, the maximum non-dimensional peak acceleration response of this sample which is equal to 51.55, is shown in Fig. 12(b).

The peak acceleration responses resulting from all simulations can be analyzed to determine their probability distribution. For example, Fig. 13 illustrates the PDF of the non-dimensional peak acceleration response for the j, k -th vibration mode of floors subjected to modal force due to different walking harmonics. The plots also show the mean values of the non-dimensional peak acceleration response of floors obtained from Monte Carlo simulations, represented by black lines. Comparing the peak acceleration response shown in Fig. 12(b) ($\ddot{p}_{h,j,k(max)} = 51.55$) for a sample with the mean value of all simulations (Fig. 13b) ($\bar{p}_{h,j,k(max)} = 72.2$), it can be observed that the peak acceleration response of this sample is lower than the mean value by approximately 33%.

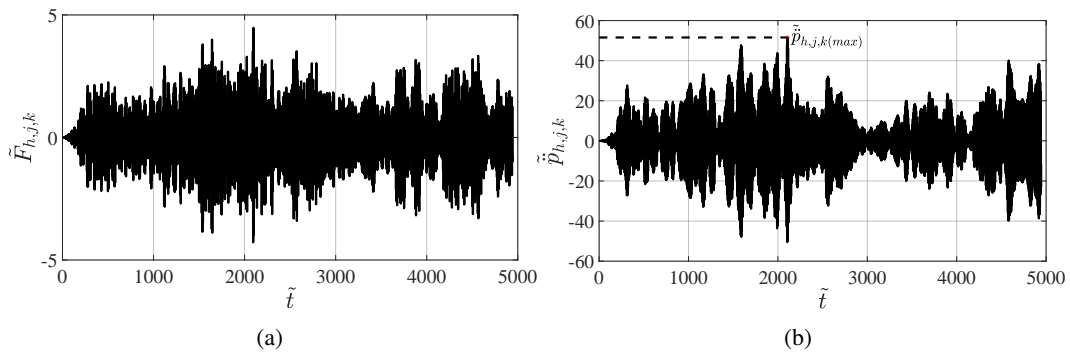


Figure 12: Non-dimensional time history of the modal force (a) and corresponding modal acceleration response (b) due to the walking harmonic h , (MLS2, $j = k = 1$, $\rho = 1$, $\mu_{\Omega_{c,1}} = 0.01$, $h = 2$, $\xi_{j,k} = 1\%$ and $N_p = 10$)

In summary, although time domain analysis provides a direct representation of the response, it is computationally expensive and may not provide a clear understanding of the underlying frequencies and modes of vibration that contribute to the response. Frequency domain analysis, on the other hand, provides a clear representation of the underlying frequencies and modes of vibration and can be more efficient than time domain analysis. Therefore, in the next section the dynamic response of floors is analyzed in frequency domain from a probabilistic point of view.

5.2. Frequency domain analysis

In this section, a spectral analysis of the dynamic response of floors under multi pedestrian walking load is carried out based on Monte Carlo simulation which allows for a more reliable and comprehensive analysis of the response, taking into account the variable nature of the multi pedestrian walking load. In this regard, 10,000 Monte Carlo simulations are performed to estimate the PSD of acceleration response of floors subjected to random multi-pedestrian walking loads. The simulations were conducted to capture the variability and uncertainty in the walking patterns and load characteristics, and the resulting PSD provides insights into the structural response under realistic pedestrian loading conditions.

In the first part of this section, the PSD of the acceleration response obtained from analytical spectral approach using the equivalent spectral model of the modal force is compared with the corresponding result obtained from numerical analysis using Monte Carlo simulation. Next, the maximum acceleration response calculated by the analytical approach is compared with the corresponding value obtained from the numerical spectral analysis.

5.2.1. PSD function of the dynamic response

The PSD of the modal force caused by walking harmonic h can be calculated based on the equivalent spectral model expressed in Eq. 38. Fig. 14 compares the PSD of the modal acceleration response obtained through numerical analysis using Monte Carlo simulations with the analytical spectral approach based on the PSD of the equivalent modal

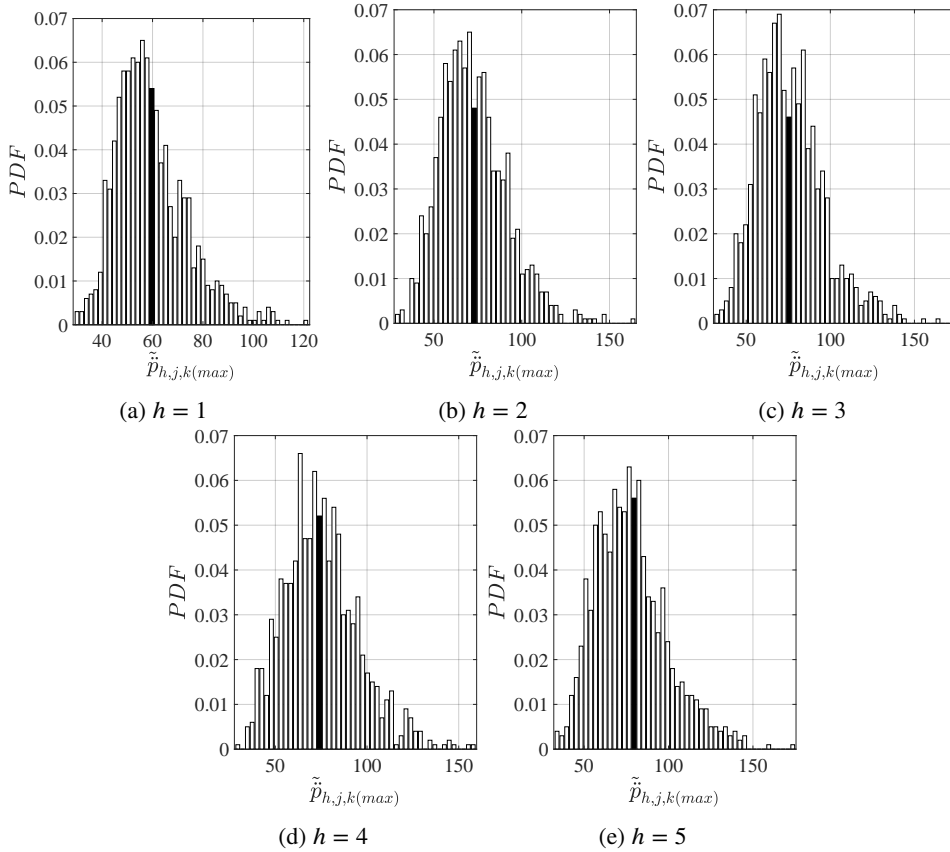


Figure 13: PDF of the non-dimensional peak acceleration responses due to different walking harmonics: (MLS2, $N_p = 10$, $\tilde{\Omega}_{c,1} = 0.01$, $\rho = 1$, $j = k = 1$, $\xi_{j,k} = 1\%$) (a) $h = 1$, (b) $h = 2$, (c) $h = 3$, (d) $h = 4$, and (e) $h = 5$

force (Eq. 38). The results demonstrate that the equivalent spectral model of the modal force is reliable for calculating the PSD function of the modal acceleration response for different walking harmonics and modal damping ratios.

The mean value of the peak acceleration response obtained through the analytical approach (Eq. 23) can be examined using the probability distribution of peak acceleration responses acquired from Monte Carlo simulations. However, prior to employing the analytical approach for estimating the mean value of the peak acceleration response (Eq. 23), it is essential to first estimate the mean value of the walking path length ($E[L_{wp}]$) according to Eq. 26. The mean value of the length of the walking paths of each pedestrian, can be estimated using Monte Carlo simulations for floors with different aspect ratios (ρ), considering different multi-pedestrian walking load scenarios. According to the results obtained from Monte Carlo simulation, the mean value of the walking path length can be estimated using the analytical expression proposed as follows:

$$\frac{E[L_{wp}]}{L_x} \cong \begin{cases} 1; & \text{(MLS1)} \\ \frac{\sqrt{2}\rho}{\rho+1}; & \text{(MLS2)} \end{cases} \quad (41)$$

Fig. 15 compares the mean value of the walking path length estimated using the Monte Carlo simulations and the analytical expression (Eq. 41) considering the loading scenario MLS2 and varying the aspect ratio in range $0.5 \leq \rho \leq 1$. The results show that the analytical expression can provide a reliable estimation of the mean value of the walking path length especially for higher values of ρ .

Dynamic response assessment of floors under multi-pedestrian walking loads: probabilistic analysis

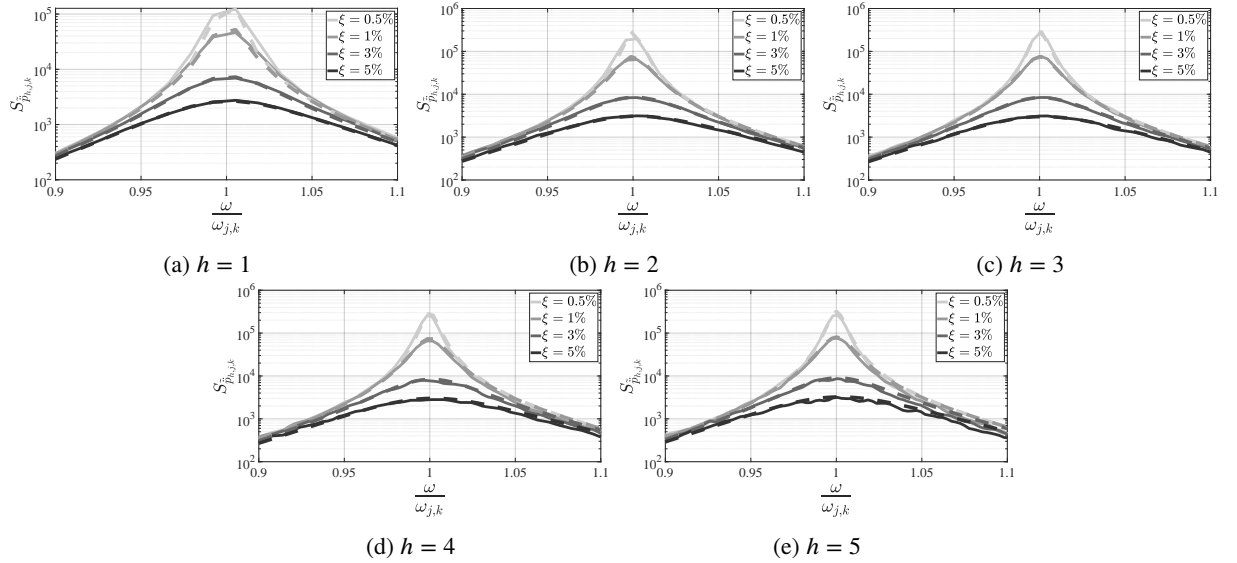


Figure 14: PSD of the non-dimensional modal acceleration response due to different walking harmonics for different modal damping ratios: comparison of the numerical (solid lines) and analytical results (dashed lines) (MLS2, $N_p = 10$, $\tilde{\Omega}_{c,1} = 0.01$, $\rho = 1$, $j = k = 1$)

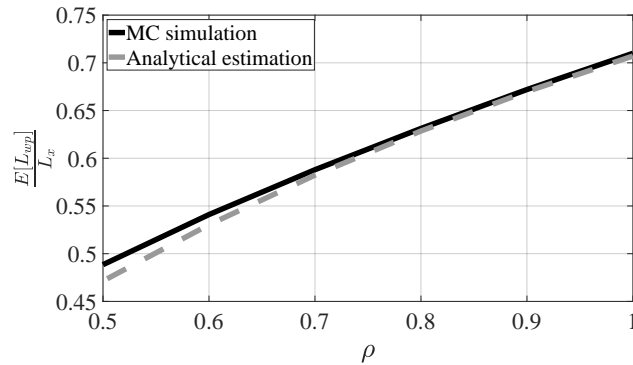


Figure 15: Mean value of the walking path length estimated by Monte Carlo simulations and analytical approach assuming the loading scenario MLS2

Fig. 16 shows the CDF of non-dimensional peak acceleration response from numerical analysis for floors with various damping ratios, superimposed with the mean peak acceleration response predicted by the analytical approach (Eq. 23) for $h = 2$ walking harmonic of multiple pedestrians. Results indicate that increasing the modal damping ratio raises the CDF value corresponding to the analytical solution's estimated mean peak acceleration response. In other words, the peak acceleration response predicted by the analytical approach is more conservative for floors with higher damping ratios.

In order to evaluate the accuracy of the analytical approach for estimating the peak acceleration response, the percentage error between the mean value of the non-dimensional peak acceleration response estimated using Eq. 23 and the corresponding value obtained through Monte Carlo simulations, is calculated as follows:

$$\text{Error (\%)} = \frac{\left[\tilde{p}_{h,j,k_{max}} \right]_{\text{Analytical}} - \left[\tilde{p}_{h,j,k_{max}} \right]_{\text{MC}}}{\left[\tilde{p}_{h,j,k_{max}} \right]_{\text{MC}}} \times 100 \quad (42)$$

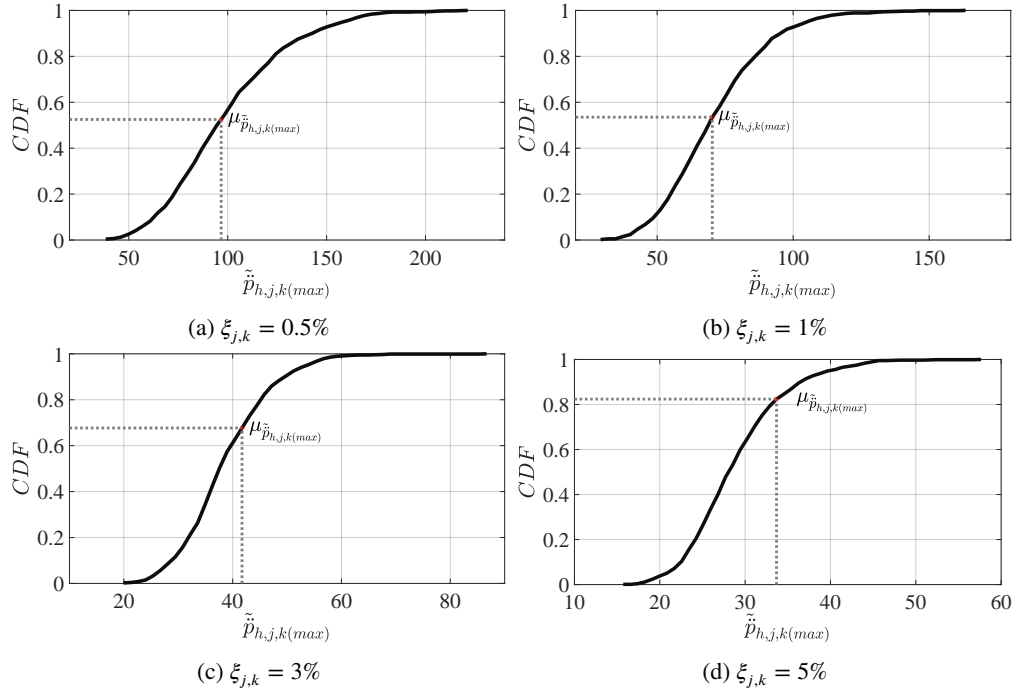


Figure 16: CDF of the non-dimensional peak acceleration response due to walking harmonic $h = 2$ with varied damping ratios and superimposition of the mean of peak acceleration estimated by analytical approach (MLS2, $N_p = 10$, $\tilde{\Omega}_{c,1} = 0.01$, $\rho = 1$, $j = k = 1$)

Fig. 17 presents the percentage error for different floors with varying modal damping ratios that are excited in resonance by different walking harmonics ($\mu_{\tilde{\Omega}_{h,j,k}} = 1$). The results indicate that the analytical approach can reliably estimate the peak acceleration response for floors with different damping ratios under resonant excitation of various walking harmonics; however, the error increases for floors with higher damping ratios.

In general, the analytical approach of estimating the mean value of peak acceleration has been shown to be effective for assessing the response of floors subjected to multi-pedestrian walking loads. The estimates of peak acceleration levels can provide guidance for the design and assessment of the floor structure.

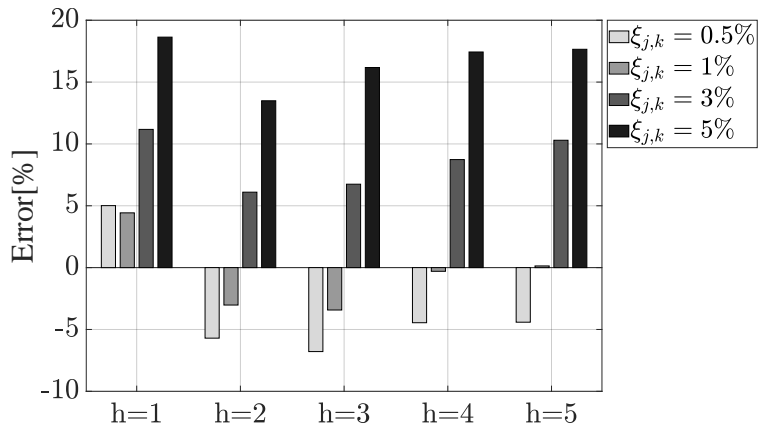


Figure 17: Percentage error in estimating the mean value of the modal non-dimensional maximum acceleration response ($\ddot{p}_{h,j,k(max)}$) for floors with different damping ratios (MLS2, $N_p = 10$, $\tilde{\Omega}_{c,1} = 0.01$, $\rho = 1$, $j = k = 1$)

6. Conclusions

In this paper, the dynamic response of rectangular floors under multiple-pedestrian walking loads was analyzed, taking into account the stochastic nature of parameters associated with both the walking path and the walking load. The PSD function of the modal force resulting from multi-pedestrian walking force was analyzed varying the involved non-dimensional parameters.

Numerical analysis of the PSD of the modal force was conducted using Monte Carlo simulations. The results indicated that the PSD of the modal force is primarily influenced by the step frequency (f_p) and walking harmonic order (h), which contribute to the variability of walking frequency. Furthermore, it was found that the parameters $\tilde{\Omega}_{c,h}$ and ρ have a negligible effect on the PSD of the walking force. On the other hand, the amplitude of the PSD of the modal force is affected by the number of pedestrians (N_p), loading scenario (represented by the coefficient of C_{wp}), pedestrian characteristics (G and α_h), and vibration mode shape.

Based on the numerical results obtained through Monte Carlo simulations, the study extended an existing spectral load model for walking multiple pedestrians, originally introduced for footbridges, to floors by incorporating the effect of multi-pedestrian loading scenarios. Then, the proposed equivalent spectral model was used to investigate the dynamic response of floors under multiple pedestrian walking loads. The findings indicated that the spectral model of the modal force can be trusted to compute the PSD function of the modal acceleration response for various modal damping ratios.

A formula was proposed to estimate the mean value of the peak acceleration response of floors. It assumed that the modal dynamic response of floors for the mode j, k is primarily resonant due to the $h - th$ harmonic. The comparison with Monte Carlo simulations has shown that the analytical approach allows to reliably estimate the mean value of the peak acceleration response for floors with different damping ratios under resonant excitation of various walking harmonics. However, the approach tended to overestimate the dynamic response for floors with higher damping ratios, resulting in increased errors. This finding is particularly significant as emphasized the damping ratio as a critical parameter in the probabilistic assessment of floors. Therefore, it is essential to carefully consider the influence of the damping ratio on the predicted vibration response.

Finally, the study proposed using the SRSS technique to calculate the total peak acceleration response of floors, assuming that the modes are widely spaced.

CRedit authorship contribution statement

Elyas Bayat: Methodology, Software, Investigation, Writing - review & editing. **Federica Tubino:** Conceptualization, Methodology, Review & Editing, Supervision.

References

- [1] Z. Muhammad, P. Reynolds, O. Avci, M. Hussein, Review of pedestrian load models for vibration serviceability assessment of floor structures, *Vibration* 2 (2018) 1–24.
- [2] A. Aloisio, D. P. Pasca, Y. De Santis, T. Hillberger, P. F. Giordano, M. M. Rosso, R. Tomasi, M. P. Limongelli, C. Bedon, Vibration issues in timber structures: A state-of-the-art review, *Journal of Building Engineering* (2023) 107098.
- [3] Z. O. Muhammad, P. Reynolds, et al., Probabilistic multiple pedestrian walking force model including pedestrian inter-and intrasubject variabilities, *Advances in Civil Engineering* 2020 (2020).
- [4] N. Cheraghi-Shirazi, K. Crews, S. Malek, Review of vibration assessment methods for steel-timber composite floors, *Buildings* 12 (2022) 2061.
- [5] Z. O. Muhammad, P. Reynolds, Vibration serviceability of building floors: performance evaluation of contemporary design guidelines, *Journal of Performance of Constructed Facilities* 33 (2019).
- [6] N. C. Van Engelen, J. Graham, Comparison of prediction and measurement techniques for pedestrian-induced vibrations of a low-frequency floor, *Structural Control and Health Monitoring* 26 (2019) e2294.
- [7] E. Bayat, F. Tubino, Dynamic response of floors induced by a single walking pedestrian including walking path variability, *Structures* 46 (2022) 1280–1292.
- [8] J. Chen, R. Xu, M. Zhang, Acceleration response spectrum for predicting floor vibration due to occupant walking, *Journal of Sound and Vibration* 333 (2014) 3564–3579.
- [9] J. Brownjohn, V. Racic, J. Chen, Universal response spectrum procedure for predicting walking-induced floor vibration, *Mechanical Systems and Signal Processing* 70 (2016) 741–755.
- [10] Z. Xie, X. Hu, H. Du, X. Zhang, Vibration behavior of timber-concrete composite floors under human-induced excitation, *Journal of Building Engineering* 32 (2020) 101744.

- [11] S. Zhang, L. Xu, Human-induced vibration of cold-formed steel floor systems: Parametric studies, *Advances in Structural Engineering* 23 (2020) 2030–2043.
- [12] Y. Cai, G. Gong, J. Xia, J. He, J. Hao, Simulations of human-induced floor vibrations considering walking overlap, *SN Applied Sciences* 2 (2020) 1–15.
- [13] O. Caballero-Garatachea, G. Juárez-Luna, M. E. R. Sandoval-Hernández, Methods for the vibration analysis of reinforced concrete precast one-way joist slab floor systems under human walking, *Journal of Building Engineering* 43 (2021) 103217.
- [14] K. Liu, L. Liu, Q. Zhu, Y. Liu, F. Zhou, Dynamic testing and numerical simulation of human-induced vibration of cantilevered floor with tuned mass dampers, in: *Structures*, volume 34, Elsevier, 2021, pp. 1475–1488.
- [15] J. Chen, M. Zhang, W. Liu, Vibration serviceability performance of an externally prestressed concrete floor during daily use and under controlled human activities, *Journal of Performance of Constructed Facilities* 30 (2016) 04015007.
- [16] O. Abdeljaber, M. Hussein, O. Avci, B. Davis, P. Reynolds, A novel video-vibration monitoring system for walking pattern identification on floors, *Advances in Engineering Software* 139 (2020) 102710.
- [17] X. Zhang, Q. Li, Y. Wang, Q. Wang, Vibration of a u-shaped steel–concrete composite hollow waffle floor under human-induced excitations, *Advances in Structural Engineering* 23 (2020) 2996–3008.
- [18] C. Wang, W.-S. Chang, W. Yan, H. Huang, Predicting the human-induced vibration of cross laminated timber floor under multi-person loadings, in: *Structures*, volume 29, Elsevier, 2021, pp. 65–78.
- [19] G. Piccardo, F. Tubino, Equivalent spectral model and maximum dynamic response for the serviceability analysis of footbridges, *Engineering Structures* 40 (2012) 445–456.
- [20] A. Ferrarotti, F. Tubino, Generalized equivalent spectral model for serviceability analysis of footbridges, *Journal of Bridge Engineering* 21 (2016) 04016091.
- [21] K. Van Nimmen, P. Van den Broeck, G. Lombaert, F. Tubino, Pedestrian-induced vibrations of footbridges: An extended spectral approach, *Journal of Bridge Engineering* 25 (2020).
- [22] E. Shahabpoor, A. Pavic, V. Racic, Structural vibration serviceability: New design framework featuring human-structure interaction, *Engineering Structures* 136 (2017) 295–311.
- [23] J. Wang, J. Chen, Y. Yokoyama, J. Xiong, Spectral model for crowd walking load, *Journal of Structural Engineering* 146 (2020) 04019220.
- [24] J. Wang, J. Chen, A comparative study on different walking load models, *Struct. Eng. Mech* 63 (2017) 847–856.
- [25] S. Chen, R. Zhang, J. Zhang, Human-induced vibration of steel–concrete composite floors, *Proceedings of the Institution of Civil Engineers-Structures and Buildings* 171 (2018) 50–63.
- [26] M. S. Gonçalves, A. Pavic, R. L. Pimentel, Vibration serviceability assessment of office floors for realistic walking and floor layout scenarios: Literature review, *Advances in Structural Engineering* 23 (2020) 1238–1255.
- [27] A. W. Leissa, The free vibration of rectangular plates, *Journal of sound and vibration* 31 (1973) 257–293.
- [28] J. W. Nicholson, L. A. Bergman, Vibration of damped plate-oscillator systems, *Journal of engineering mechanics* 112 (1986) 14–30.
- [29] L. Fryba, C. Steele, Vibration of solids and structures under moving loads, *J. Appl. Mech* 43 (1976) 524.
- [30] J. W. Smith, *Vibration of structures: applications in civil engineering design*, 1988.
- [31] S. Timoshenko, S. Woinowsky-Krieger, et al., *Theory of plates and shells*, volume 2, McGraw-hill New York, 1959.
- [32] A. K. Chopra, *Dynamics of structures*, Pearson Education India, 2007.
- [33] I. Elishakoff, *Probabilistic theory of structures*, Courier Corporation, 1999.
- [34] A. G. Davenport, Note on the distribution of the largest value of a random function with application to gust loading., *Proceedings of the Institution of Civil Engineers* 28 (1964) 187–196.
- [35] A. Der Kiureghian, Structural response to stationary excitation, *Journal of the Engineering Mechanics Division* 106 (1980) 1195–1213.
- [36] S. Živanović, A. Pavić, P. Reynolds, Probability-based prediction of multi-mode vibration response to walking excitation, *Engineering structures* 29 (2007) 942–954.
- [37] G. Piccardo, F. Tubino, Simplified procedures for vibration serviceability analysis of footbridges subjected to realistic walking loads, *Computers & structures* 87 (2009) 890–903.
- [38] J. S. Bendat, A. G. Piersol, *Random data: analysis and measurement procedures*, John Wiley & Sons, 2011.
- [39] G. Piccardo, F. Tubino, Dynamic response of euler-bernoulli beams to resonant harmonic moving loads, *Structural Engineering and Mechanics* 44 (2012) 681–704.